

Band-structure, optical properties, and defect physics of the photovoltaic semiconductor SnS

Julien Vidal, Stephan Lany, Mayeul d'Avezac, Alex Zunger, Andriy Zakutayev, Jason Francis, and Janet Tate

Citation: [Applied Physics Letters](#) **100**, 032104 (2012); doi: 10.1063/1.3675880

View online: <http://dx.doi.org/10.1063/1.3675880>

View Table of Contents: <http://scitation.aip.org/content/aip/journal/apl/100/3?ver=pdfcov>

Published by the [AIP Publishing](#)

Articles you may be interested in

[Non-monotonic effect of growth temperature on carrier collection in SnS solar cells](#)

Appl. Phys. Lett. **106**, 203901 (2015); 10.1063/1.4921326

[Structural and electronic modification of photovoltaic SnS by alloying](#)

J. Appl. Phys. **115**, 113507 (2014); 10.1063/1.4868974

[Electronic and optical properties of Ga₃-xIn₅+xSn₂O₁₆: An experimental and theoretical study](#)

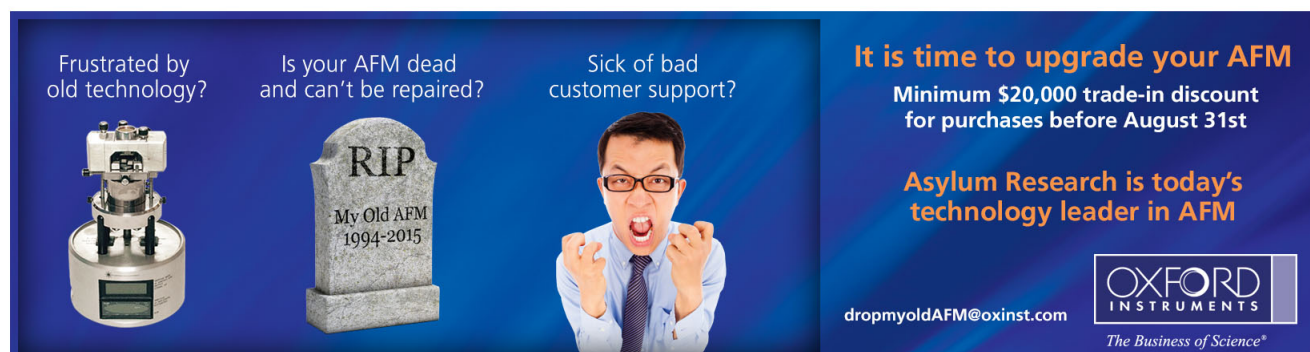
J. Appl. Phys. **115**, 013703 (2014); 10.1063/1.4861130

[Electrical and thermoelectrical properties of SnTe-based films and superlattices](#)

Appl. Phys. Lett. **95**, 122106 (2009); 10.1063/1.3236541

[Temperature-dependent structural and optical properties of SnS films](#)

J. Appl. Phys. **101**, 093522 (2007); 10.1063/1.2729450

The advertisement is set against a dark blue background with a subtle light pattern. It features three main visual elements: a photograph of an old, bulky AFM on the left; a grey tombstone in the center with the inscription 'RIP My Old AFM 1994-2015'; and a man in a white shirt and tie, shouting with his hands raised in frustration on the right. Text is arranged around these elements to promote an upgrade to Asylum Research technology. On the right side, there is a logo for Oxford Instruments and their tagline 'The Business of Science®'. The overall tone is one of urgency and dissatisfaction with current technology.

Frustrated by old technology?

Is your AFM dead and can't be repaired?

Sick of bad customer support?

It is time to upgrade your AFM

Minimum \$20,000 trade-in discount for purchases before August 31st

Asylum Research is today's technology leader in AFM

dropmyoldAFM@oxinst.com

OXFORD
INSTRUMENTS

The Business of Science®

Band-structure, optical properties, and defect physics of the photovoltaic semiconductor SnS

Julien Vidal,¹ Stephan Lany,^{1,a)} Mayeul d'Avezac,¹ Alex Zunger,^{1,b)} Andriy Zakutayev,^{2,c)} Jason Francis,² and Janet Tate²

¹National Renewable Energy Laboratory, Golden, Colorado 80401, USA

²Department of Physics, Oregon State University, Corvallis, Oregon 97331, USA

(Received 25 September 2011; accepted 6 December 2011; published online 17 January 2012)

SnS is a potential earth-abundant photovoltaic (PV) material. Employing both theory and experiment to assess the PV relevant properties of SnS, we clarify on whether SnS has an indirect or direct band gap and what is the minority carrier effective mass as a function of the film orientation. SnS has a 1.07 eV indirect band gap with an effective absorption onset located 0.4 eV higher. The effective mass of minority carrier ranges from 0.5 m_0 perpendicular to the van der Waals layers to 0.2 m_0 into the van der Waals layers. The positive characteristics of SnS feature a desirable p-type carrier concentration due to the easy formation of acceptor-like intrinsic Sn vacancy defects. Potentially detrimental deep levels due to Sn_S antisite or S vacancy defects can be suppressed by suitable adjustment of the growth condition towards S-rich. © 2012 American Institute of Physics. [doi:10.1063/1.3675880]

Earth abundancy is considered to be a major criterion for a photovoltaic (PV) absorber that has a potential not only to reach the terawatt energy production goal but also sustain it.¹ The achievement of such a goal in the case of two of the most promising thin-film technologies (i.e., CdTe (Ref. 2) and Cu(In,Ga)Se₂ (Ref. 3)) is under question due to cost and supply issues of In, Ga, and Te,⁴ as well as the toxicity and associated disposal requirements for Cd. Attempts have been made to replace scarce and expensive indium in Cu(In,Ga)Se₂ (CIGS) by zinc and tin and forming Cu₂(ZnSn)(SSe)₄ (CZTS),⁵ in some cases quite successfully.⁶ However, theoretical investigations have revealed several important issues with CZTS,⁷ most of which originate from multi-valence of Sn and narrow stability range of this multicomponent material.^{8,9} Therefore, simpler binary Earth-abundant absorbers such as SnS,^{10–13} FeS₂,¹⁴ and Cu_{2–x}S (Ref. 15) have recently experienced a renewed interest in the PV community.

SnS is a potential photovoltaic absorber because of its high optical absorption above the photon energy threshold of 1.3 eV,^{10,16} which is close to the optimal band gap.¹⁷ SnS shows further an intrinsic p-type conductivity with carrier concentrations in the range 10¹⁵–10¹⁸ cm^{–3},^{10,16,18} which is suitable for PV absorbers. However, SnS-based heterojunction solar cells have so far achieved rather low efficiency of below 2%,¹⁰ which could be due to an intrinsic material limitation or due to the lack of proper device optimization, e.g., the band alignment at the heterojunction between SnS and the buffer/contact.¹⁹ In this letter, we studied the basic PV relevant properties of SnS both theoretically and experimentally, so as to assess its potential for future PV thin-film technologies. Our band structure calculation predicts that SnS has an indirect band gap of 1.07 eV and an effective absorp-

tion threshold for a SnS thin film at 1.4–1.5 eV. While the carrier effective masses are rather anisotropic due to the layered structure (see Fig. 1), small calculated electron masses $m_{\perp}^e = 0.1\text{--}0.2 m_0$ should allow good minority carrier transport properties within the layer planes. The defect calculations suggest that the intrinsic p-type conductivity is due to the easy formation of Sn vacancies which act as shallow acceptors. The Sn-on-S antisite defect is a donor and has potentially detrimental deep defect levels, but can be avoided under S-rich growth conditions. In light of these findings, we conclude that there is still considerable potential to improve SnS-based PV devices.

In order to assess the defect physics of SnS, we performed total-energy defect calculations and effective mass calculations, all employing projector augmented wave implementation of the VASP code (Ref. 20) within density functional theory (DFT) using 72 atom supercells. We tested both local density approximation (LDA) and the generalized gradient Approximation (GGA) for the exchange-correlation functional of DFT, finding that LDA describes the structural and elastic parameters considerably better than GGA, which is typical for van der Waals-bonded layered crystal structure.²¹ The calculated *a*-axis lattice constant and the bulk moduli are (*a* = 11.01 Å and *B* = 41.1 GPa) and (*a* = 11.55 Å and *B* = 20.1 GPa) in LDA and GGA, respectively, compared to experimental values (*a* = 11.2 Å and *B* = 36.6 GPa).²² Thus, we are using here the LDA for all total-energy calculations. Since some defect formation energies show a considerable dependence on the interlayer distance, we further constrain *a*-axis lattice constant to the experimental value. The usual corrections for finite supercell size effects have been applied,²³ and the defect and carrier concentration have been determined by solving numerically the self-consistency condition for defect concentrations and the Fermi level under the requirement of overall charge neutrality.²⁴ In order to improve the Sn and S chemical potentials which enter the evaluation of the defect formation energy, we used the fitted elemental reference energy method of Ref. 25, considering Sn-S phases

^{a)}Author to whom correspondence should be addressed. Electronic mail: stephan.lany@nrel.gov.

^{b)}Present address: University of Colorado, Boulder, Colorado 80309, USA.

^{c)}Present address: National Renewable Energy Laboratory, Golden, Colorado 80401, USA.

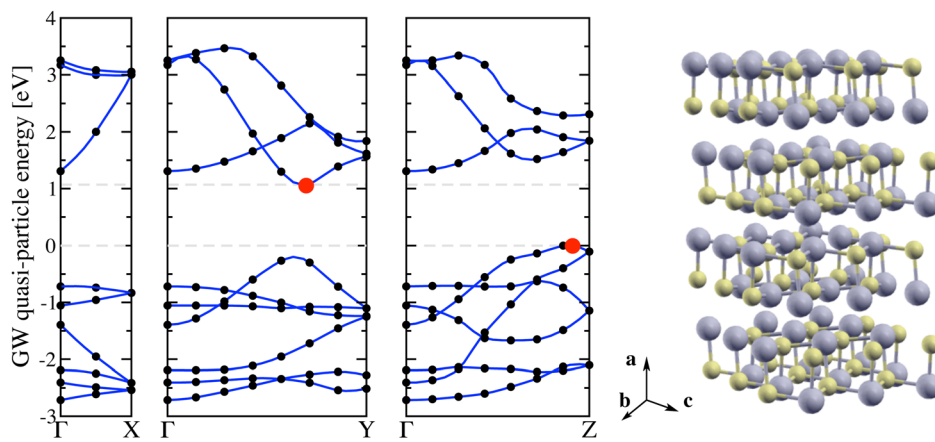


FIG. 1. (Color online) Calculated band structure of SnS along Γ -X (along **a**-axis), Γ -Y (along **b**-axis), and Γ -Z (along **c**-axis). Large red dots represent valence band maximum and conduction band minimum. Crystal structure of SnS: small yellow spheres represent S atoms, while large grey spheres represent Sn atoms.

SnS, SnS₂, Sn₂S₃. The latter phases are considered to define the growth condition together with the calculated heat of formation of SnS $\Delta H_f = \Delta\mu_{\text{Sn}} + \Delta\mu_{\text{S}}$: S-rich ($\Delta\mu_{\text{S}} = -0.27$ eV, $\Delta\mu_{\text{Sn}} = -0.93$ eV) and Sn-rich ($\Delta\mu_{\text{S}} = -1.2$ eV, $\Delta\mu_{\text{Sn}} = 0$ eV). The band structure, effective masses, and optical spectrum were determined for the experimental lattice parameters on a $4 \times 15 \times 14$ **k**-point grid using the GW method derived from many body perturbation theory and implemented as of Ref. 26, and the method of Ref. 27 for the calculation of the dielectric function including electron-hole interaction (excitonic effects). For the GW calculations, we employ a scheme that consistently predicts accurate band gaps over a wider range of II-VI and III-V semiconductors.²⁸ The GW quasiparticle energy shifts relative to the underlying GGA calculations are approximately uniform throughout the Brillouin zone and increase the band gap by 0.32 eV without changing the location of the band edges in reciprocal space. For the excitonic effects, we used a constant screening factor $1/\epsilon_\infty$ for the electron-hole exchange, where $\epsilon_\infty = 13$ is the calculated dielectric constant.

SnS thin films of 200–400 nm thickness were prepared by pulsed laser deposition (PLD) from a sulfur-rich Sn-S target (S/Sn = 1.5–2.0) using 1 J/cm² laser beam (248 nm) operating at 3–10 Hz. The temperature of fused silica (*a*-SiO₂) substrates positioned in an ultra-high vacuum chamber (10^{-9} Torr base pressure– 10^{-3} Torr of Ar) at 5 cm distance from the target was varied between 300 °C and 500 °C. The composition, structure, optical, and transport properties of the films were studied by electron-probe microanalysis (EPMA), x-ray diffraction (XRD), optical absorption spectroscopy, and Van der Pauw Hall effect measurements, respectively. We also note that the depositions results were reproducible over the time scale of more than 1 yr and over different PLD system operators.

The SnS thin films grown on *a*-SiO₂ have preferential (100) orientations indicated by dominance of (*H*00) XRD peaks in the θ -scan and confirmed by the results of χ -scan through the (131) peak. Thus, the van der Waals bonded SnS layers are stacked parallel to the substrate, which can be considered either beneficial (chemically inactive surface) or detrimental (mechanical instability) to PV applications of this material. The Sn/S ratio of the thin films was determined to be close to unity within measurement error of EPMA.

According to our GW calculation, SnS has an indirect band gap of 1.07 eV, in agreement with early characteriza-

tions,¹⁸ but contrasting common perceptions that SnS is a direct gap semiconductor.^{10,16,19} Fig. 1 shows the band structure along different high symmetry directions. The effective masses of holes along *a*, *b*, and *c* axes ($m_a^h = 1.5 m_0$, $m_b^h = 0.21 m_0$, and $m_c^h = 0.33 m_0$) are anisotropic, with the largest effective mass perpendicular to van der Waals planes, as observed experimentally.¹⁸ Our predicted electron masses ($m_a^e = 0.5 m_0$, $m_b^e = 0.13 m_0$, and $m_c^e = 0.2 m_0$) are smaller and less anisotropic than the holes masses. While the in-plane masses $m_\perp^e = 0.1$ – $0.2 m_0$ are slightly larger but comparable with other PV absorbers like GaAs, CdTe, or Cu(In,Ga)Se₂, the out-of-plane mass $m_\parallel^e = 0.5 m_0$ is significantly larger, suggesting that minority carrier transport in SnS is hindered by the preferential (100) growth direction of polycrystalline thin-films.

In indirect semiconductors, the weak phonon assisted absorption requires a considerable thickness of the material for complete absorption (for example, the typical absorber thickness of c-Si solar cells is $\sim 200 \mu\text{m}$). In the present SnS thin-films of less than $1 \mu\text{m}$ thickness, the absorption is dominated by direct allowed optical transitions, which were considered for calculation of the theoretical absorption spectrum. As shown in Fig. 2, the calculated absorption reproduces the measured spectrum very well when excitonic effects are included. For solar cell applications with a typical film thickness of $1 \mu\text{m}$, the absorption coefficient needs to be about 2 – $3 \times 10^4 \text{ cm}^{-1}$ for complete photon absorption, which is achieved at photon energy above about 1.5 eV. Thus, there is an offset of about 0.4 eV between the effective absorption

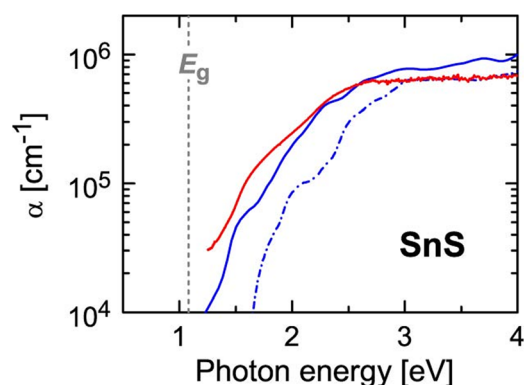


FIG. 2. (Color online) Measured (light red) and calculated (dark blue) absorption spectra of SnS, with (solid) and without (dashed) excitonic effects.

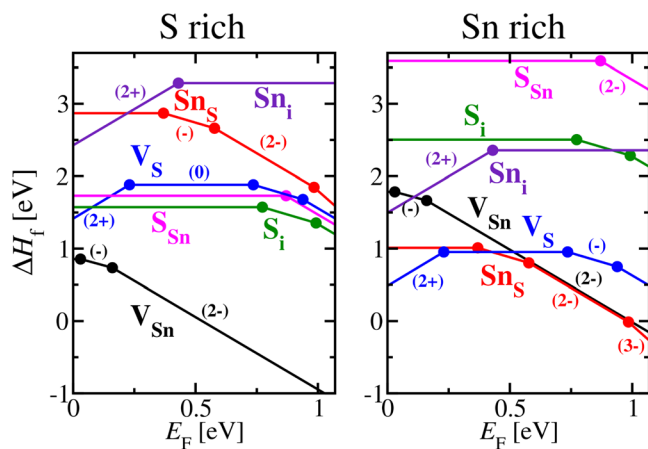


FIG. 3. (Color online) Calculated defect formation enthalpies for intrinsic defects in S-rich (left panel) and Sn-rich (right panel) limits in SnS.

threshold and the band gap, which is considerably larger than in direct-gap absorbers, typically ~ 0.1 eV in GaAs, CdTe, or CuInSe₂.²⁹ This offset is undesirable because the energy difference is lost to thermalization of electrons and holes.

As shown in Fig. 3, out of the 6 basic intrinsic defects in SnS (2 vacancies, 2 antisites, and 2 interstitials), 3 have a sufficiently small formation enthalpy to significantly affect the electrical properties. The tin vacancy (V_{Sn}) acts as a shallow acceptor and is mainly responsible for the p -type conductivity of SnS. In the Sn-rich limit, the sulfur vacancy (V_{S}) has lower formation enthalpy than V_{Sn} , but it does not significantly compensate the p -type conductivity due to V_{Sn} , because the ultra-deep transition level $(2+/0)$ of V_{S} lies very close to the valence band maximum and, therefore, does not compensate the holes produced by V_{Sn} . In the $2+$ state of V_{S} , there occurs an interesting atomic relaxation effect, where one Sn atom undergoes a relaxation along the a -axis into the interlayer space. Such relaxation effects are the main reason for the above mentioned sensitivity to interlayer spacing. The increased nearest neighbor distance and depleted s -like partial charge of the relaxing Sn atom can be attributed to a change into the $+IV$ oxidation state, similar to observations made for Cu₂ZnSnS₄.⁷ Similarly to Cu(In,Ga)Se₂,³⁰ the S vacancy in SnS has negatively charged states inside the band gap which could act as electron traps. Moreover, $(2+/0)$ transition of V_{S} is significantly less deep than in Cu(In,Ga)Se₂ and could potentially act as detrimental deep gap states such as Sn-on-S antisite (Sn_{S}) which has a low formation energy and deep transition levels. Those defects can, however, be avoided by using S-rich conditions defined by the phase coexistence between SnS and Sn₂S₃, under which its formation energy is considerably increased (see Fig. 3). Since, in practice, it will be desirable to avoid the coexistence of secondary S-rich phases like Sn₂S₃ or SnS₂, it is advisable to adjust the growth not too much towards S-rich conditions, so that these phases remain suppressed.

Fig. 4 shows the calculated and measured hole concentrations at room temperature as a function of the growth temperature. The theoretical carrier density is maximal under the S-rich condition and minimal under the Sn-rich condition, and increases with increasing growth temperature. The measured

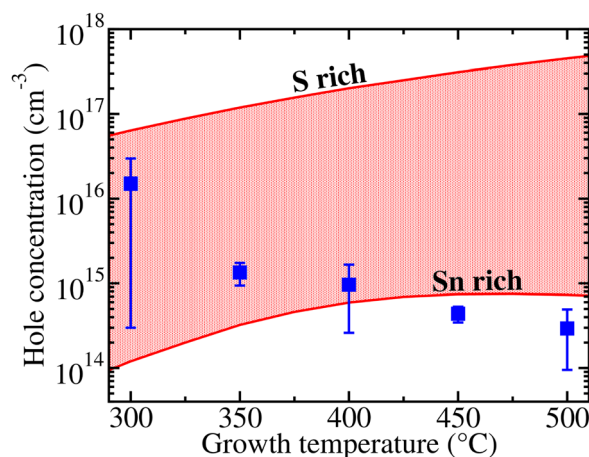


FIG. 4. (Color online) Measured (blue squares) and calculated (red lines) hole concentrations between the limiting Sn-rich and S-rich growth conditions.

carrier density spans about the same range $p \sim 10^{14}$ – 10^{17} cm⁻³. The lowest achieved experimental hole concentration (3×10^{14} cm⁻³ at 500 °C deposition temperature) is somewhat smaller than the values typically reported in literature (10^{15} – 10^{18} cm⁻³).^{10,16,18} Reported hole concentration values and corresponding error bars were determined from measurements performed on many samples deposited under varying Ar pressure, repetition rate, target-substrate distance, and cooling rate deposition parameters that determine kinetics of the growth. Small error bars for the depositions above 300 °C substrate temperature suggest that the film growth in this temperature region is governed by thermodynamics rather than kinetics, and thus, resulting carrier concentrations can be compared to theoretical predictions for the thermodynamic equilibrium conditions. Compared to the theory result, we observe the opposite trend with increasing growth temperature, which can be attributed to the fact that higher temperatures lead to increasingly sulfur poor growth conditions due to high volatility of sulfur. Loss of sulfur in pulsed laser deposition is a quite common phenomenon observed for sulfides³¹ and sulfur-based mixed-anion compounds.³² We further measured reasonably large Hall mobilities (between 4 and 16 cm²/Vs) for the motion of holes within the plane of SnS layers. Due to the large predicted effective mass in the perpendicular direction (see above), however, the hole mobility must be expected to be smaller in this direction by about a factor of three, assuming constant scattering time.

Based on the present theoretical and experimental study, we suggest that SnS has some potential as an inexpensive, earth-abundant absorber material. Disadvantages are the indirect nature of the band gap and the relatively large carrier effective masses due to the layered crystal structure. On the positive side are the intrinsic p -type doping at desirable concentrations due to V_{Sn} defects and the absence of detrimental deep centers when grown under suitable conditions.

The theoretical part of this work was funded by the U.S. Department of Energy, Office of Energy Efficiency and Renewable Energy, under Contract No. DE-AC36-08GO28308 to NREL. The use of massively parallel computing capabilities

at the National Energy Research Scientific Computing Center is gratefully acknowledged. The experimental part of this work was supported by the National Science Foundation of USA under Grant No. DMR-0804916.

- ¹C. Wadia, A. P. Alivisatos, and D. M. Kammen, *Environ. Sci. Technol.* **43**, 2072 (2009).
- ²J. Britt and C. Ferekides, *Appl. Phys. Lett.* **62**, 2851 (1993).
- ³I. Repins, M. A. Contreras, B. Egaas, C. DeHart, J. Scharf, C. L. Perkins, B. To, and R. Noufi, *Prog. Photovoltaics* **16**, 235 (2008).
- ⁴Critical Materials Strategy, U.S. Department of Energy, 2010.
- ⁵H. Katagiri, *Thin Solid Films* **480**, 426 (2005).
- ⁶T. K. Todorov, K. B. Reuter, and D. B. Mitzi, *Adv. Mater.* **11**, E156 (2010).
- ⁷K. Biswas, S. Lany, and A. Zunger, *Appl. Phys. Lett.* **96**, 201902 (2010).
- ⁸A. Redinger, D. M. Berg, P. J. Dale, and S. Siebentritt, *J. Am. Chem. Soc.* **133**, 3320 (2011).
- ⁹T. Tanaka, A. Yoshida, D. Saiki, K. Saito, Q. Guo, M. Nishio, and T. Yamaguchi, *Thin Solid Films* **518**, S29 (2010).
- ¹⁰K. T. Ramakrishna Reddy, N. Koteswara Reddy, and R. W. Miles, *Sol. Energy Mater. Sol. Cells* **90**, 3041 (2006).
- ¹¹K. Hartman, J. L. Johnson, M. I. Bertoni, D. Recht, M. J. Aziz, M. A. Scarpula, and T. Buonassisi, *Thin Solid Films* **519**, 7421 (2011).
- ¹²R. W. Miles, O. E. Ogah, G. Zoppi, and I. Forbes, *Thin Solid Films* **517**, 4702 (2009).
- ¹³P. Sinsermsuksakul, J. Heo, W. Noh, A. S. Hock, and R. G. Gordon, *Adv. Energy Mater.* **1**, 1116 (2011).
- ¹⁴L. Yu, S. Lany, R. Kykyneshi, V. Jieratum, R. Ravichandran, B. Pelatt, E. Altschul, H. A. S. Platt, J. F. Wager, D. A. Keszler *et al.*, *Adv. Energy Mater.* **1**, 748 (2011).
- ¹⁵A. Ashour, J. Optoelectron. Adv. Mater. **8**, 1447 (2006).
- ¹⁶H. Noguchi, A. Setiyadi, H. Tanamura, T. Nagatomo, and O. Omoto, *Sol. Energy Mater. Sol. Cells* **35**, 325 (1994).
- ¹⁷W. Schockley and H. J. Queisser, *J. Appl. Phys.* **32**, 510 (1961).
- ¹⁸W. Albers, C. Haas, H. J. Vink, J. D. Wasscher, *J. Appl. Phys.* **32**, 2220 (1961).
- ¹⁹M. Sugiyama, Y. Murata, T. Shimizu, K. Ramya, C. Venkataiah, T. Sato, K. T. R. Reddy, *Jpn. J. Appl. Phys.* **50**, 05HF03 (2011).
- ²⁰G. Kresse and J. Joubert, *Phys. Rev. B* **59**, 1758 (1999).
- ²¹V. V. Ivanovskaya, A. Zobelli, A. Gloter, N. Brun, V. Serin, and C. Colliex, *Phys. Rev. B* **78**, 134104 (2008).
- ²²L. Ehm, K. Knorr, P. Dera, A. Krimmel, P. Bouvier, and M. Mezouar, *J. Phys.:Condens. Matter.* **16**, 3545 (2004).
- ²³S. Lany and A. Zunger, *Phys. Rev. B* **78**, 235104 (2008).
- ²⁴S. Lany, Y.-J. Zhao, C. Persson, and A. Zunger, *Appl. Phys. Lett.* **86**, 042109 (2005).
- ²⁵S. Lany, *Phys. Rev. B* **78**, 245207 (2008).
- ²⁶M. Shishkin and G. Kresse, *Phys. Rev. B* **75**, 235102 (2007).
- ²⁷J. Paier, M. Martijn, and G. Kresse, *Phys. Rev. B* **78**, 121201 (2008).
- ²⁸S. Lany, P. Graf, M. D'Avezac, A. Zunger (unpublished). We start the GW calculation based on GGA wavefunctions and iterate the quasiparticle energies until convergence. We include local-field effects within DFT,27 and use for d-states an on-site potential that corrects for the typical overestimation of the d-band energies in GW.
- ²⁹*Handbook of Optical Constants of Solids II*, edited by E. D. Palik (Academic, San Diego, 1985).
- ³⁰S. Lany and A. Zunger, *J. Appl. Phys.* **100**, 113725 (2006).
- ³¹P. F. Newhouse, P. A. Hersh, A. Zakutayev, A. Richard, H. A. S. Platt, D. A. Keszler, and J. Tate, *Thin Solid Films* **517**, 2473 (2009).
- ³²A. Zakutayev, D. H. McIntyre, G. Schneider, R. Kykyneshi, D. A. Keszler, C. H. Park, and J. Tate, *Thin Solid Films* **518**, 5494 (2010).